3. Wells, C. & Bagshaw, C. R. *Nature* **313,** 696–697 (1985).
4. Chantler, P. D. & Szent-Györgyi, A. G. *J. molec. Biol.* **138,** 473–492 (1980).
5. Wallimann, T. Szent-Györgyi, A. G. *Biochemistry* **20,** 1176–1187 (1981).
6. Kwon, H. *et al. Proc. natn. Acad. Sci. U.S.A.* **87,** 4771–4775 (1990).
7. Szentkiralyi, E. M. *J. Muscle Res. Cell Motil.* **5,** 147–164 (1984).
8. Fromherz, S. & Szent-Györgyi, A. G. *Biophys. J.* **64a,** 7 (1993).
9. Rayment, I. *et al. Science* **261,** 50–58 (1993).
10. Ikura, M. *et al. Science* **256,** 632–638 (1992).
11. Meador, W. E., Means, A. R. & Quiocho, F. A. *Science* **257,** 1251–1255 (1992).
12. Mercer, J. A., Seperack, P. K., Strobel M. C., Copeland, N. G. & Jenkins, N. A. *Nature* **349,** 709–713 (1991).
13. Cheney, R. J. & Mooseker, M. S. *Curr. Opin. Cell Biol.* **4,** 27–35 (1992).
14. Persechini, A. & Kretsinger, R. H. *J. biol. chem.* **263,** 12175–17178 (1988).
15. Collins, J. H. *J. Muscle Res. Cell Motil.* **12,** 3–25 (1991).
16. Kretsinger, R. H. & Nockolds, C. E. *J. biol. Chem.* **248,** 3313–3326 (1973).
17. Bennett, A. G. & Bagshaw, C. R. *Biochem. J.* **233,** 173–179 (1986).
18. da Silva, A. C. R. & Reinach, F. C. *Trends biochem. Sci.* **16,** 53–57 (1991).
19. Strynadka, N. C. J. & James, M. N. *Curr. Opin. struct. Biol.* **1,** 905–914 (1991).
20. Szent-Györgyi, A. G. & Chantler, P. D. in *Myology* Vol. 2 (eds Engel, A. G. & Franzini-Armstrong, C.) 506–528 (McGraw-Hill, New York, 1994).
21. Sellers, J. R., Chantler, P. D. & Szent-Györgyi, A. G. *J. Molec. Biol.* **144,** 223–245 (1980).
22. Rowe, T. & Kendrick-Jones, J. *EMBO J.* **11,** 4715–4722 (1992).
23. Hardwicke, P. M. D., Wallimann, T. & Szent-Györgyi, A. G. *Nature* **301,** 478–482 (1983).
24. Trybus, K. M. & Chatman, T. A. *J. biol. Chem.* **268,** 4412–4419 (1993).
25. Vibert, P. & Cohen, C. *J. Musc. Res. Cell Motility* **9,** 296–305 (1988).
26. Rayment, I. *et al. Science* **261,** 58–65 (1993).
27. Wells, J. A. & Yount, R. G. *Meth. Enzym.* **85,** 93–116 (1982).
28. Berchtold, H. *et al. Nature* **365,** 126–132 (1993).
29. Kjeldgaard, M., Nissen, P., Thirup, S. & Nyborg, J. *Structure* **1,** 35–50 (1993).
30. Wang, B.-C. *Meth. Enzym.* **115,** 90–112 (1985).
31. Jones, T. A., Zou, J. Y., Cowan, S. W. & Kjeldgaard, M. *Acta crystallogr.* A**47,** 110–119 (1991).
32. Kabsch, W., Mannherz, H. G., Suck, D., Pai, E. F. & Holmes, K. C. *Nature* **347,** 37–44 (1990).
33. Brünger, A. T. *X-PLOR v. 3.0 Manual* (Yale Univ., New Haven, 1992).
34. Stafford, W. F., Szentkiralyi, E. M. & Szent-Györgyi, A. G. *Biochemistry* **24,** 5273–5280 (1979).
35. Funk, M. O., Nakagawa, Y., Skochdopole, J. & Kaiser, E. T. *Int. J. Pept. Prot. Res.* **13,** 296–303 (1979).
36. Kraulis, P. J. *J. appl. Crystallogr.* **24,** 946–950 (1991).
37. Sekharudu, C. Y. & Sundaralingam, M. *Prot. Sci.* **2,** 620–625 (1993).

ACKNOWLEDGEMENTS. We thank G. A. Petsko and D. Ringe for discussion and encouragement, D. Wiley and S. Harrison for access to their area detector, S. Burley and J. Kuriyan for hospitality and assistance, and P. Vibert and R. Kretsinger for discussion. This work was supported by grants from the NIH and Muscular Dystrophy Association (C.C. and A.S-G.) and by the Alexander von Humboldt Gesellschaft (I.S.). D.H.H. was supported by a grant from the NIH to G. A. Petsko and a grant from the Lucille P. Markey Charitable Trust to D. Ringe. Diffraction data were collected at Brookhaven National Laboratory in the Biology Department single-crystal diffraction facility at beamline X12-C in the National Synchrotron Light Source (supported by the US Department of Energy, Office of Health and Environmental Research and by the NSF. This article is dedicated to the memory of Eva M. Szentkiralyi.

LETTERS TO NATURE

A map of a collisionally evolving dust disk around Fomalhaut

S. Alan Stern*, Michel C. Festou† & David A. Weintraub‡

* Space Sciences Department, Southwest Research Institute, 6220 Culebra Road, San Antonio, Texas 78238, USA
† Observatoire Midi-Pyrénées, 14 avenue E. Belin, F-31400 Toulouse, France
‡ Department of Physics and Astronomy, Vanderbilt University, Nashville, Tennessee 37235, USA

THE presence of dust around normal (main-sequence) stars is a possible signature of the early stages of planet formation. Scattered light from the star β Pictoris provides evidence of a dust disk extending out to about 1,000 astronomical units[1], and the observation of far-infrared excess emission from several other main-sequence stars[2] suggests the presence of orbiting cold dust grains[3]. Because the dynamical lifetime of this dust is short, it is thought to be supplied and replenished by collisions among a population of comets or asteroids[4–8]. Observations by Chini *et al.*[9,10] of β Pic and several other infrared-excess stars at a wavelength of 1.3 mm have supported the idea that they are surrounded by extended dust disks. Techniques developed recently now permit imaging at these wavelengths, and we have used these techniques to obtain a map of the dust disk around the nearby, prototypical infrared-excess star Fomalhaut with a spatial resolution of 80 AU. This image provides direct confirmation that the dust is distributed in a disk-like structure, and shows that the structure extends about 200 AU from the star, farther than estimated previously[9,10]. We estimate that a high rate of cometary and/or asteroidal collisions is required to maintain this disk.

Electromagnetic radiation from a typical main-sequence star is very nearly that of an ideal, isothermal black body. Each main-sequence stellar type has a unique temperature, characteristic of the thin, photospheric region from which it emits most of its light. From measurements at visual wavelengths, one can determine the photospheric temperature of a star and thereby directly calculate the amount of emission the star will produce as a function of wavelength. Certain stars, specifically those in the process of either forming or dying, are commonly surrounded by substantial amounts of fine-grained cold material. During the ~90% of a star's lifetime which it spends on the main-sequence, however, the stellar environment is normally free of microscopic dust particles. The infrared-excess stars discovered by the Infrared Astronomy Satellite (IRAS) are main-sequence stars characterized by as much as an order of magnitude more emission at far-infrared wavelengths than predicted from their photospheric black-body profiles. The most likely source for this far-infrared excess radiation has convincingly been shown to be orbiting dust grains heated by the star[2]. Because the dynamical lifetime of this dust is short, an underlying population of comets or asteroids undergoing mutual collisions is implied. As such, it is widely believed that studies of these far-infrared-excess systems provide information about the processes and timescales involved in planetary-system formation and/or evolution.

Although no successor space mission (that studies the far-infrared) to IRAS has yet flown, Chini *et al.*[9,10], and Zuckerman and Becklin[7,8] have pioneered the use of the longer-wavelength submillimetre and millimetre wavelength ground-based windows to make important advances. But previous work on IRAS infrared-excess stars (such as theirs) has relied on point-flux observations made along the lines of sight to these stars. With the advent of bolometer arrays in the millimetre-wavelength range, it has now become possible to map the emission around these stars, and therefore further refine knowledge about the spatial distributions and masses of their cool dust structures. We made observations of Fomalhaut (α PsA; A3V; $D = 6.7$ pc) at the Institut de Radio Astronomie Millimétrique (IRAM) telescope at Pico Veleta, Spain on 19–20 February 1993 UT, at an effective wavelength of 1.3 mm, and in excellent, very dry weather. We used the Max-Planck-Institut für Radioastronomie seven-channel bolometer[11], the beams of which are arranged in a hexagon surrounding a central channel. At 1.3 mm, each beam operates with a diffraction-limited half power beam width (HPBW) of 12 arcsec, corresponding to 80 AU at Fomalhaut. The centre-to-centre separation of the bolometer beams is 22 arcsec (150 AU). Because most of the observed flux in any astronomical millimetre-wave bolometer measurement is thermal emission from Earth's 100 K atmosphere, we adopted the standard procedure of using a chopping secondary mirror to remove the telluric sky signal. The secondary mirror was set to produce a chop throw of 45 arcsec at a chop frequency of 2.0 Hz. For our flux calibrator, Uranus, we adopted a 1.3-mm brightness temperature of 97.5 K (refs 12, 13). Observations of Uranus were used to calculate a system noise equivalent flux density of 80 mJy $Hz^{-1/2}$ per channel, in good agreement with that quoted (90 mJy $Hz^{-1/2}$ per channel) in the nominal observing performance specifications for the array.

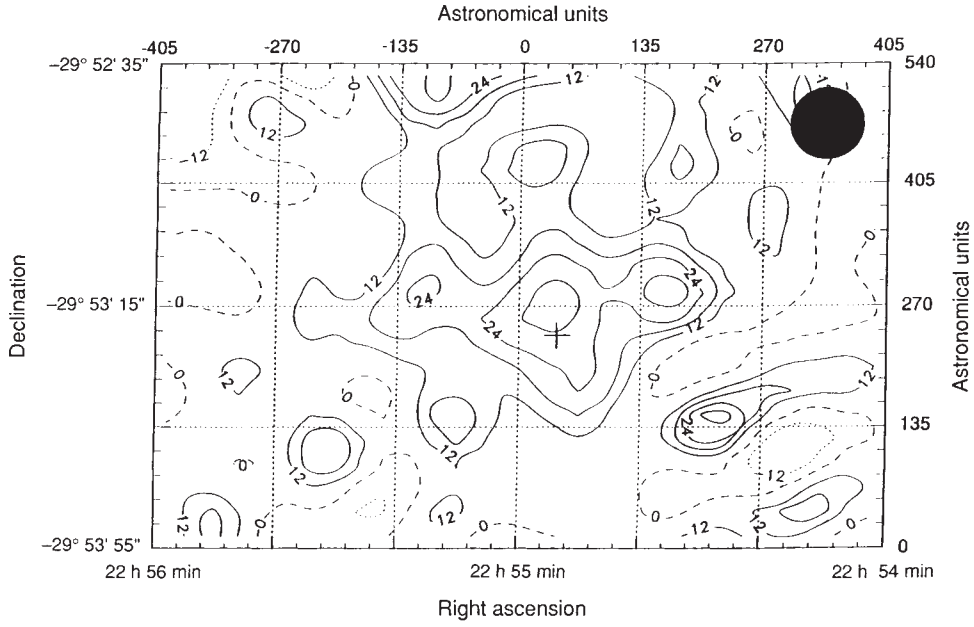

FIG. 1 A co-added, 120 × 80 arcsec, 1.3-mm-wavelength map of the region around Fomalhaut made at IRAM; north is at the top, east to the left. The edges of the larger, 3 × 2 arcmin maps are not displayed because they were not uniformly sampled, as the central region is (see text). Fomalhaut's 1993 position is indicated by the small cross at the centre. The large black disc at the upper right represents the IRAM beam size at a wavelength of 1.3 mm (12 arcsec HPBW). There is no significant signal in the map below -1σ (-12 mJy); thus the noise level is well illustrated with the $\pm 1\sigma$ ($+12$ mJy, solid line; -12 mJy, dashed line) contours. Higher contours are drawn at 0.5σ intervals (18, 24 and 30 mJy). The 0-mJy contour is shown with a dashed line to illustrate the flatness of the subtracted baseline. The three prominent peaks near the map centre are separated by intervals of ~22 arcsec, which is close to (but not the same as) the spacing of the bolometer detectors; further, these three peaks do not form the hexagonal pattern of the detectors, and are not in the bolometer scan direction. We conclude they are real. The map was made in azimuth/elevation coordinates over 2.7 h, during which the airmass of Fomalhaut ranged between 2.5 and 3.1. Proper pointing was verified between maps. The sky transmission was measured three times using a standard skydip procedure. This revealed an essentially constant 1.3-mm zenith optical depth of $\tau_{1.3} = 0.13 \pm 0.01$ during the observations. The instrument was operated at highest gain for maximum sensitivity. The three maps of the Fomalhaut area were individually cleaned, reduced to right ascension/declination coordinates, and converted to calibrated flux using the IRAM NOD2 software package[23,24]. Single-pixel data glitches (or 'spikes') above the 3-σ level were removed. The three co-registered maps were co-added and a fitted background plane was removed. This slightly tilted background plane was constrained not to remove flux at the location of Fomalhaut. The prominent feature at the centre of the map is the extended emission feature resulting from Fomalhaut's extended dust ensemble. Minor peaks in the map with lower fluxes and much smaller solid angles are due to either statistical noise and/or map edge effects.

Accurate pointing for each observation of Fomalhaut was ensured by offsetting to the position of the star after using a gaussian fit routine to centre and focus on the nearby (1°N) source 2255−282, the position of which has been well-established (G. Sandell, manuscript in preparation). Routine pointing checks revealed reliable performance with <3 arcsec (two-axis r.m.s.) pointing errors. Three, 3 × 2 arcmin maps were obtained by raster scanning the array over the field around Fomalhaut at an angular velocity of 4 arcsec s^{-1}, with cross-scan direction steps of one-half beam (6 arcsec). An unsmoothed, S/N-weighted co-addition of our three maps is shown in Fig. 1. (S/N is the signal-to-noise ratio). The 120 × 80 arcsec area shown in Fig. 1 is the fully-sampled portion of the full (180 × 120) arcsec map areas; partial sampling near the edges occurs because only some of the seven beams are on the map area along its edges.

Figure 1 reveals a roughly elliptical emission region centred on the 1993 position of Fomalhaut. The peak 1.3-mm emission detected toward Fomalhaut is 32 ± 12 mJy, along the line of sight to the star. The 1σ error level of 12 mJy per beam in our data (taken at high air mass but in optimum weather) compares well with the predicted sensitivity of 8 mJy. The total flux detected above the 18-mJy contour surrounding Fomalhaut is 305 ± 80 mJy (a 3.8σ detection of the extended emission). Owing to its proper motion, Fomalhaut has moved 16.8 arcsec since 1950.0. The centre of the 32-mJy isophote surrounding the peak emission corresponds (within 0.5 arcsec in right ascension and 6 arcsec in declination) to the proper-motion-corrected position of Fomalhaut. At the S/N of our data, this one-half beamwidth offset is not statistically significant. The close correspondence between the emission peak in the map and the position of the star is strong evidence that we detected radiation from dust around Fomalhaut, rather than from a randomly superimposed background source.

It is important to point out that this extended emission is not due to Fomalhaut's photosphere. This is because the flux from Fomalhaut's 8,800 K photosphere is a point source 10^4 times smaller than the IRAM beamsize, with a predicted flux of <1 mJy, and is not detectable with present-day millimetre-wavelength-techniques. As such, we conclude that the millimetre-emission region mapped around Fomalhaut is due to thermal emission from dust surrounding this main-sequence infrared-excess star. With this detection, this dust assemblage surrounding Fomalhaut becomes an important analogue to that surrounding the well-known IRAS infrared-excess star β Pictoris (A5V, $D = 16.7$ pc), which was mapped in scattered light almost a decade ago[1]. Our 1.3-mm-wavelength map confirms and significantly extends earlier results[5,7–10,14,15] which inferred (but did not directly detect) extended emission around Fomalhaut. The 18-mJy contour in Fig. 1 suggests that the emission source probably extends at least 190 AU from Fomalhaut in the east and west directions, but appears to be unresolved in the north–south direction. On the sky, the detected 18-mJy emission contour subtends 1 arcmin in the east–west direction. Although the S/N per beam of this detection is too low to make strong quantitative statements about the geometry and total flux density of the extended source, future observations with more integration time should make this possible. More-sensitive observations should also reveal whether the disk is more extended at lower flux levels than we can reliably measure in this first-detection.

As noted above, all past measurements of submillimetre- and millimetre-wavelength emission along the line of sight to Fomalhaut have been made with single-channel bolometers making point-observations. The net flux measured by that technique is the difference between the flux measured along the line of sight and the flux measured at the chop position, which is implicitly assumed to be zero. With this technique Chini *et al.*[9,10] obtained

7.3 ± 2.2 mJy at a wavelength of 1.3 mm with a 12-arcsec HPBW and a 30-arcsec chop throw at IRAM. The same workers later detected three times as much flux, 21 ± 2.5 mJy, at 1.3 mm with a 24-arcsec HPBW and a 70-arcsec chop throw at the 15-m Swedish-ESO Submillimetre Telescope (SEST) observatory.

Our map reveals a flux along the central line of sight to Fomalhaut that appears to be higher than, but not inconsistent with, the extended emission region detected in past non-mapping observations[7–10]. The additional flux we detected is present outside the central region. The extended nature of the Fomalhaut emission apparently revealed by the 1.3-mm map suggests that some of the point-observations of Fomalhaut made in the past may have 'chopped away' and/or missed flux outside their line-of-sight beams. This hypothesis is supported by the fact that Chini *et al.* found a larger flux[10] in their larger beam experiment at SEST, which is consistent with their IRAM measurements only if Fomalhaut is extended at a wavelength of 1.3 mm compared to the 12 arcsec HPBW of the IRAM measurement. Given this finding, we suggest that disk properties of Fomalhaut and other infrared-excess stars studied by point-bolometer work at submillimetre–millimetre wavelengths require re-evaluation using mapping techniques. This finding has recently been described in detail[16].

To estimate the total dust mass detected in the disk around Fomalhaut revealed in Fig. 1, we assume the dust grain opacity is described by a power law in frequency[17]

$$\kappa_\nu = \kappa_0 \left(\frac{\nu}{\nu_0} \right)^\beta$$

where κ_0 is the value of the dust grain opacity at a reference frequency ν_0. Next, following Sandell and Weintraub[16], we use eqn (6) of Hildebrand[17] to write an expression for the dust mass, $M_{\rm dust}$:

$$M_{\rm dust} = 3.76 \times 10^{20} \left(\frac{1{,}200}{\nu} \right)^{3+\beta} \times F_\nu (e^{0.048\nu/T_{\rm dust}} - 1) D^2 \text{ grams}$$

where ν is the frequency in GHz, F_ν is the flux in mJy, $T_{\rm dust}$ is the dust temperature in K, the distance D is in pc, and we adopted $\kappa_0 = 10.0$ cm^2 g^{-1} at $\nu_0 = 1{,}200$ GHz (that is, 250 μm). This expression assumes that the emission from dust at 1.3 mm wavelength is optically thin, but does not assume that the spectrum is on the Rayleigh–Jeans tail. The optically thin assumption is strongly supported by previous IRAS and millimetre wavelength studies of Fomalhaut[3].

For an integrated flux density of 305 mJy and a typical dust temperature of 43 K (expected 100 AU from Fomalhaut; the stellar luminosity $L_* = 6.7\, L_\odot$, where $L_\odot$ is the stellar luminosity), we estimate a dust mass of $M_{\rm dust} = 2.3 \times 10^{26} \times 5.2^\beta$ g. We use $\beta = 0$ and $\beta = 2$ to obtain minimum and maximum estimates of $M_{\rm dust}$. This gives the range $4.4 \times 10^{26} < M_{\rm dust} < 1.2 \times 10^{28}$ g, or ~0.07–2 $M_{\rm earth}$. Variations in the dust temperature between 30 and 100 K (as appropriate for distances of 20 to 200 AU) do not change the results by more than a factor of two. These mass estimates indicate that the mass of Fomalhaut dust detected at a wavelength of 1.3 mm is at least 10^5 times more than the interplanetary dust cloud of the Solar System[19].

Now consider the timescales for loss of dust from the Fomalhaut system. The dominant dynamical loss mechanism beyond ~60 AU is Poynting–Robertson (P–R) drag. P–R drag limits the lifetime of low-eccentricity grains to $\sim 1 \times 10^6\, R_{100}^2 r \rho_{2.0}$ yr, where R_{100} is the astrocentric semi-major axis in units of 100 AU, r is the grain radius in micrometres, and $\rho_{2.0}$ is the grain density in units of 2.0 g cm^{-3}. For the estimated stellar age of Fomalhaut, $2 \pm 0.7 \times 10^8$ yr (ref. 20), the P–R lifetime of 30-μm grains 100 AU from Fomalhaut is 0.15 times the present age of Fomalhaut. Smaller grains are removed even faster. Even at 200 AU, the P–R lifetime for 30-μm grains against P–R drag is less than the estimated age of the star. For millimetre-sized particles, the P–R transport lifetime can approach the age of Fomalhaut at 200 AU. But using a robust "particle in a box" model[6,21,22], it is possible to show that collisions between millimetre-sized grains in the system will remove these particles on orbits with eccentricities exceeding 1% on timescales of 10^6–10^7 yr, even at 200 AU. The short grain lifetimes indicated by these simple calculations provide strong circumstantial evidence for recent dust production around Fomalhaut, at least for the region inside 200 AU of interest here.

Conservatively taking 5×10^7 yr as a relevant dust-loss timescale, the steady-state production rate of dust needed to supply the mass of the observed Fomalhaut disk implies a total loss of 2×10^{27} to 5×10^{28} g (0.3–8 $M_{\rm earth}$) over the age of the star. As 1.3-mm observations are not sensitive to either the mass locked up in large bodies (which have low surface-area to mass ratios) or in micrometre-sized grains (which are inefficient emitters at millimetre wavelengths), these dust loss and total-disk-mass estimates represent lower limits.

Because the lifetime of the observed dust is short compared to the age of Fomalhaut, it is natural to invoke an embedded population of planetesimals undergoing collisions as a mechanism to produce the observed dust. If we assume a typical instantaneous dust mass of ~10^{27} g and a dynamical lifetime of 5×10^7 yr, a dust production rate of 2×10^{19} g yr^{-1} is implied. This is equivalent to 25–100 comet Halley masses (each ~1–4×10^{17} g) being ground up each year. This rate of collisions is 10^2–10^3 times the rate of cometary collisions occuring in the present-day Kuiper disk surrounding the Sun[21,22]. Recognizing the high rate of collisions implied by the dust resupply rates required at Fomalhaut, we suggest that its disk is still rapidly evolving from its formation state to a less-massive remnant disk (like our Kuiper comet disk[22]). Whether planets have already formed, or are now accumulating from the colliding bodies around Fomalhaut, is an exciting area for future investigation. □

Received 9 December 1993; accepted 7 February 1994.

1. Smith, B. A. & Terrile, R. J. *Science* **226,** 1421–1424 (1984).
2. Aumann, H. H. *et al. Astrophys. J.* **278,** L23–L27 (1984).
3. Backman, D. E. & Paresce, F. in *Protostars and Planets III* (eds Levy, E. & Lunine, J. I.) 1253–1304. (Univ. of Arizona Press, Tucson, 1993).
4. Weissman, P. R. *Science* **224,** 987–989 (1984).
5. Harper, D. A., Lowenstein, R. F. & Davidson, D. A. *Astrophys. J.* **285,** 808–820 (1984).
6. Stern, S. A. *Icarus* **84,** 447–466 (1990).
7. Zuckerman, B. & Becklin, E. E. in *Submillimetre Astronomy* (eds Watt, G. D. & Webster, A. S.) 147–153 (Klüwer, Dordrecht, 1993).
8. Zuckerman, B. & Becklin, E. E., *Astrophys. J.* **414,** 793–802 (1993).
9. Chini, R., Krugel, E. & Kreysa, E. *Astr. Astrophys.* **227,** L5–L11 (1990).
10. Chini, R., Krugel, E., Shustov, B., Tutokov, A. & Kreysa, E. *Astr. Astrophys.* **252,** 220–228 (1991).
11. Kreysa, E., Lemke, R., Haslam, C. G. T. & Sievers, A. W. *Astr. Astrophys.* (in the press).
12. Griffin, M. J. *et al. Icarus* **65,** 244–258 (1986).
13. Orton, G. S. *et al. Icarus* **67,** 289–301 (1986).
14. Gillet, F. C. in *Light on Dark Matter* (ed. Israel, F. P.) 61–69 (Reidel, Dordrecht, 1986).
15. Aumann, H. H. in *The Infrared Spectra of Stars* (Pergamon, New York, 1990).
16. Weintraub, D. A. & Stern, S. A. *Astr. J.* (submitted).
17. Hildebrand, R. H. *Q. Jl. R. astr. Soc.* **24,** 267–282 (1983).
18. Sandell, G. & Weintraub, D. A. *Astr. Astrophys.* (submitted).
19. Sykes, M. V. *et al.* in *Asteroids II* (eds Binzel, R. P., Gehrels, T. & Matthews, M. S.) 336–368 (Univ. of Arizona Press, Tucson, 1989).
20. Green, E. M., Demarque, P. & King, C. R. *The Revised Yale Isochrones and Luminosity Functions* (Yale Univ. Obs., New Haven, 1987).
21. Stern, S. A. & Stewart, G. R. *Bull. Am. Astr. Soc.* **26,** 1064 (1993).
22. Stern, S. A. & Stewart, G. R. *Icarus* (submitted).
23. Haslam, C. T. G. *Astr. Astrophys. Suppl. Ser.* **15,** 333–350 (1974).
24. Salter, C. J. *IRAM Preprint* No. 84 (Institut de Radio Astronomie Millimétrique, Grenoble, 1986).

ACKNOWLEDGEMENTS. We thank the staff of the IRAM observatory for their assistance. We particularly thank A. Sievers for assistance with the IRAM NOD2 bolometer image-recovery package. D. Backman, J. Bally and M. Duncan provided comments on the manuscript. G. Sandell provided us with a list of millimetre pointing sources in advance of publication. This work was supported by NASA, the NRAO (S.A.S) and IRAM (for M.F.C.).